



Article

Ethyne Furan Ratios as Indicators of High and Low Temperature p-PAH Emissions from Household Stoves in Haryana India

Robert M. Weltman ¹, Rufus D. Edwards ^{1,*} , Norbert Staimer ², Ajay Pillarisetti ³, Narendra K. Arora ⁴ 
and Sergey A. Nizkorodov ⁵ 

¹ Department of Environmental and Occupational Health, University of California Irvine, Irvine, CA 92697, USA

² BioAssayPro LLC, La Jolla, CA 92037, USA

³ School of Public Health, University of California Berkeley, Berkeley, CA 94720, USA

⁴ INCLEN Trust International, New Delhi 110020, India; nkarora@incentrust.org

⁵ Department of Chemistry, University of California Irvine, Irvine, CA 92697, USA

* Correspondence: edwardsr@uci.edu

Abstract: Emission factors of 16 particle-bound polycyclic aromatic hydrocarbons (16 p-PAHs) from residential fuel combustion are highly variable, resulting in significant uncertainty with respect to the estimation of emissions of PAHs from this sector. Emissions of 16 p-PAHs were characterized during daily cooking activities for two traditional Indian cookstoves: the angithi, which burns dung, and the chulha, using brushwood, dung, and a mix of brushwood and dung fuels. Previous work has shown that ethyne–furan ratios are reasonable predictors of high- and low-temperature pyrolysis that explain most of the variability in volatile organic compound (VOC) emissions from biomass burning. Here, we demonstrate that, as the ethyne–furan ratio increases in these stoves, the 2- and 3-ring p-PAHs account for a smaller fraction of summed 16 p-PAHs and emissions of high molecular weight p-PAHs and elemental carbon (EC) increase. This indicates a shift from less to more fused ring p-PAHs, leading to higher EC emissions. Similar to studies of VOC emissions from biomass burning, 16 p-PAH emissions from the same stove type varied widely and were not related to modified combustion efficiency, thus suggesting that larger numbers of field studies are required to adequately capture these emissions using inventories. In addition, in these stoves, fluoranthene and pyrene ratios used in source apportionment overlap with ratios typically used to identify fossil-fuel burning and thus do not adequately constrain these sources.

Keywords: polycyclic aromatic hydrocarbons; emission factors; solid fuel; biomass cookstoves; India



check for updates

Academic Editor: Ferdinando Salata

Received: 12 December 2024

Revised: 13 January 2025

Accepted: 18 January 2025

Published: 23 January 2025

Citation: Weltman, R.M.; Edwards, R.D.; Staimer, N.; Pillarisetti, A.; Arora, N.K.; Nizkorodov, S.A. Ethyne Furan Ratios as Indicators of High and Low Temperature p-PAH Emissions from Household Stoves in Haryana India. *Atmosphere* **2025**, *16*, 121. <https://doi.org/10.3390/atmos16020121>

Copyright: © 2025 by the authors. Licensee MDPI, Basel, Switzerland. This article is an open access article distributed under the terms and conditions of the Creative Commons Attribution (CC BY) license (<https://creativecommons.org/licenses/by/4.0/>).

1. Introduction

Approximately three billion individuals worldwide live in households that primarily cook with solid fuels, which represents 90% of rural households and approximately 50% of all households worldwide [1]. In South Asia, combustion of solid fuels for residential heating and cooking results in elevated levels of PM_{2.5} in households [2], neighborhoods [3], and urban areas [1,3,4] and is a major emission source of particulate polycyclic aromatic hydrocarbons (p-PAHs). The p-PAHs emitted from cooking with solid fuels are involved in both non-malignant and, after biotransformation, malignant diseases of the airways [5], adverse reproductive health outcomes [6], and pose a significant health concern from solid

fuel exposures [7]. The 16 p-PAHs measured in this study are designated as high-priority pollutants by the United States Environmental Protection Agency (US EPA) due to their health risks and prevalence and persistence in the environment. Indoor air concentrations of 16 p-PAHs have generally been reported to be higher than outdoor concentrations [8], and present an exposure risk to women and young infants [7]. The regional implications of these emissions are less well known, as p-PAH emissions from solid fuel use span several orders of magnitude in existing inventories [9].

There have been very few field assessments of PAH emissions from traditional stoves in rural Indian households [7,10–13]. The majority of studies reporting emission factors (EFs) and source diagnostic ratios of PAHs have been estimated using controlled burns from fuels in laboratory tests, which have been widely reported as not representative of emissions during typical household use [12,14–18]. For example, EFs for PAHs from household solid fuel burning indoors were 4–6 times higher than EFs from burning similar fuels in test chambers. In addition, EFs were highly variable between homes, with standard deviations > 50% of emission values as a result of stove type and cooking practices that are not well represented by laboratory burns [9,19]. Variability in these EFs has been ascribed to a number of factors, including the high fuel moisture content, the design of cook stoves, and the burning phase of fuel during testing [9]. The temperature of the reaction and the physical characteristics of the biopolymer control which pyrolysis mechanism is the main source of emitted volatile organic compounds (VOCs) from biomass burning. Recent work has demonstrated that ethyne–furan ratios, as markers for high (>500 °C) and low-temperature pyrolysis (300–500 °C), explain most of the variability in VOC emissions from biomass burning [20]. Further, ethyne–furan ratios were better predictors of VOC emissions from cookstoves when compared to non-pyrolysis based metrics such as modified combustion efficiency (MCE), as the temperature of the pyrolysis process drives differences in VOC profiles from distinct combustion events [20]. Pyrolysis products such as eugenol, typical of lignin decomposition to substituted propylphenols, are highly sooting, which indicates that the pyrolysis fingerprint of a fuel is a contributing factor to the rate of soot formation during combustion [21]. For p-PAH, as temperatures increase, it is generally understood that lower molecular weight smaller p-PAH compounds transition to larger, generally more mutagenic p-PAHs, and finally to coagulated soot particles that form EC [22].

Diagnostic ratios of p-PAHs have been frequently used in source apportionment studies of ambient PM to apportion PAHs to biomass burning, vehicular emissions, and other sources in either household or direct emissions [23,24] and in downwind atmospheric concentrations [25–27], as the ratios of individual species are considered fairly stable during atmospheric transport [23,25]. Apportioning sources, for example, by diagnostic ratios or principal component analyses [8,9], relies on well-constrained PAH isomer ratios for separating source signatures [18,28,29]. PAH isomer ratios are often applied to PAHs that are close together in molecular weight, such as fluoranthene and pyrene (FLA and PYR), as the transition to higher-molecular-weight PAHs is associated with differences in combustion that can be considered intrinsic to the burn [25,26,30–32]. PAH isomer ratios of FLA to the sum of FLA and PYR (FLA/FA + PYR) in the range of 0.5 ± 0.1 are typically associated with vehicle emissions. Wood combustion diagnostic ratios vary widely across stoves, with diagnostic ratios ranging from ~0.1 to ~0.8 [30]. Parent PAH compounds have been widely used to detect PAHs from combustion, for example, in order to gauge the contribution from petroleum versus other combustion sources [31].

The analyses presented in this paper demonstrate that high-molecular-weight 16 p-PAH and elemental carbon (EC) emissions from wood, bovine dung, and mixture of both fuels in in-field measurements of chulha and angithi stoves cooking typical meals

are well predicted by the proportion of high- to low-temperature combustion. In addition, the analyses demonstrate that diagnostic ratios used to apportion sources of 16 p-PAHs in ambient PM are not sufficiently constrained to accurately separate source signatures in the context of these cookstove tests.

2. Methods

Samples were collected between August and September 2015 in a rural Indian village located at the SOMAARTH Demographic, Development, and Environmental Surveillance Site in Palwal District, Haryana, India, run by the International Clinical Epidemiological Network (INCLLEN). Pictures of the stoves in use are provided in the supplementary information (Figures S1 and S2). The chulha is a traditional U-shaped cookstove usually made with baked clay where fuels are loaded in the front and cookware placed on top. The angithi is typically used to simmer milk or animal feed and is a bowl shape also made of baked clay where animal dung patties are loaded around the bowl and an ember placed in the center before the large pot is placed over the dung patties limiting airflow. Both stoves utilize small amounts of fire starters, in this case plastic bags, to begin combustion. The plastic bags, dung patties, and wood were locally sourced from the village where measurements were performed.

More information on the field measurements can be found elsewhere [14,33,34]. Briefly, a local woman was recruited to cook 36 traditional meals for 4 people (average household size) in an outdoor kitchen in the village of Khatela, Palwal, Haryana, using the chulha with either rice or chapatti (an Indian flatbread) as starch, vegetables, and dahl based on market availability. Each meal was prepared by the same local cook who was instructed to cook typical daily village meals rather than food for special occasions. Fuel types consisting of dung ($n = 10$), brushwood ($n = 14$), or both mixed together ($n = 12$), and moisture content were predetermined, but fuel loading, fire-tending, and fuel mixture ratios of dung and brushwood were determined by the cook according to cooking preference. No other instructions regarding cooking were given to the cook to better represent typical cooking patterns. In an additional nine cooking tests, the angithi stove was used to simmer animal fodder. The molecular composition of particles was reported in Fleming et al. [33], gas phase VOC emissions were reported in Fleming et al. [34], SOA formation from these VOCs was reported in Rooney et al. [3], and Weltman et al. [14] discussed climate effects and contrasts between in-field versus laboratory emissions testing.

2.1. Sample Collection

Details on sample preparation, collection, and storage are reported in Fleming et al. [34]. Briefly, emissions were sampled in the plume 1 m above the stove. Quartz filters were used to collect PM_{2.5} samples using a flow rate of 1.5 L min⁻¹ (PCXR-8, SKC Inc., Pittsburgh, PA, USA) through cyclone samplers (2.5 micron, URG corporation, Chapel Hill, NC, USA). Flows were evaluated before and after sampling using a mass flowmeter (TSI 4140) and the average flow rate combined with the elapsed time was used to calculate sample volume. Background samples were collected on quartz filters at the same flow rates, but no PAHs above the limits of detection were observed and background subtractions were not performed. No PAHs above the limits of detection were observed in the solvent blanks used in this project. Filters were sealed after collection and kept at $-20\text{ }^{\circ}\text{C}$ in the INCLLEN field offices then moved to UCI for storage at $-80\text{ }^{\circ}\text{C}$ at the end of the measurement campaign to minimize the PAH volatilization loss which may bias results towards lower emissions [35].

Quartz filters were removed from storage at $-80\text{ }^{\circ}\text{C}$ and a 1 cm square punch was taken with a SP-10 sample punch (Sunset Laboratory Inc., Tigard, OR, USA) for elemental

carbon/organic carbon (EC/OC) analysis. The remaining filter was then placed in individual 15 mL polypropylene centrifuge tubes (Corning, Corning, NY, USA) and stored at -80°C until extraction and analysis of PAHs.

2.2. HPLC Methods

PAHs were analyzed using established HPLC methods [36]. First, 5 mL aliquots of HPLC-grade acetonitrile (Thermo Fischer Scientific, Waltham, MA, USA) were added to the centrifuge tubes containing the quartz filters via autopipette. Each centrifuge tube was then placed in a water bath sonicator (FS30 Ultrasonic Cleaner, Thermo Fisher Scientific, Waltham, MA, USA) in ice water for 45 min without being submerged. After sonication, each tube was placed into a centrifuge (IEC Centra CL3R, Thermo Fisher Scientific, Waltham, MA, USA) at 4000 rpm for 5 min. Finally, 1 mL of these extracts were filtered using a $0.2\ \mu\text{m}$ syringe filter (polyvinylidene fluoride PVDF syringe filters, $0.22\ \mu\text{m}$ pores, 13 mm diameter, Luer-Lok/Luer Slip, Tisch Scientific, Cleves, OH, USA) and placed in autosampler vials (amber glass vials with screw tops, Shimadzu, Kyoto, Japan) for analysis by high-performance liquid chromatography with a fluorescence detector (HPLC-FLD). The HPLC separations were carried out using a Hewlett Packard pump system (HP 1100 Series) connected to a diode-array detector (Hewlett Packard, HP 1050 Series, Palo Alto, CA, USA). The data were collected and integrated by HP Chem Station for LC, A.06 Revision (Hewlett Packard). An Aquasil C18 column was employed for separation ($250 \times 4.6\ \text{mm}$ I.D., $5\ \mu\text{m}$ particles, Western, Analytical Products, Inc., Murrieta, CA, USA). The injection volume was $50\ \mu\text{L}$, the flowrate $0.7\ \text{mL}/\text{min}$, and detection was performed at 254 nm. The mobile phase consisted of acetonitrile/ H_2O (70:30 *v/v*). Concentrations in each amber glass vial were calculated using a six-level linear calibration curve at 1:10, 1:50, 1:100, 1:150, 1:250, and 1:500 dilutions of a $10\ \mu\text{g}/\text{mL}$ 16-PAH analytical standard (47940-U Supelco, Millipore Sigma, St Louis, MO, USA) with duplicate injections of the 1:10, 1:150, and 1:500 dilutions ($R^2 > 0.9999$). The limits of detection were between 1.8 and 22.1 ng/mL for each PAH species in solution, calculated by multiplying the standard deviation of the intercept divided by the slope of the calibration curve by a factor of 3.3. Due to co-elution, acenaphthene and fluorene, benzo(b)fluoranthene, and benzo(k)fluoranthene, and 1,2-benzanthracene and chrysene were not resolved separately. Acenaphthylene and benzo[ghi]perylene were not well resolved or quantified in this study. Particle-bound PAHs were evaluated in a standard reference material (Standard Reference Material 1648a, Urban Particulate Matter) and recoveries were generally good for PAHs with 3 or more rings (Table S3). As a quality control check, two sets of quartz filters were also spiked in triplicate with 1 mL of a prepared $50\ \text{ng}/\text{mL}$ PAH Standard Mix (47940-U Supelco, Millipore Sigma, St. Louis, MO, USA), and after 15 min or 24 h sealed in the dark at room temperature were extracted and analyzed by HPLC-FLD following NIOSH Method 5506 to evaluate recovery. Because PAH recoveries were acceptably high ($>60\%$ and less than $<110\%$, Table S4) after 15 min, no adjustments were made to our values presented here. After 24 h at room temperature, lower molecular weight PAHs were mostly absent (Table S4). Fourteen PAHs are reported here: naphthalene (NAP), acenaphthene/fluorene (ACE/FLO), phenanthrene (PHE), anthracene (ANT), fluoranthene (FLA), pyrene (PYR), 1,2-benzanthracene/chrysene (BaA/CHY), benzo(b)fluoranthene/benzo(k)fluoranthene (BbK/BkF), benzo(a)pyrene (BaP), dibenz(a,h)anthracene (DahA), and indeno(1,2,3-c,d)pyrene (IcdP). For comparisons between stove/fuel combinations, one-way analyses of variance (1-way ANOVA) followed by Tukey's honest significance tests were used.

2.3. Sample Detection

Sample p-PAHs were above the limit of detection (LOD; between 2 and 22 ng/mL depending on species) for 45 out of 46 cooking events. In the 45 tests where PAHs were detected, 93% of individual PAH species were detected above the limit of detection (Table S1). For tests in which a measured PAH level was below LOD, the minimum ratio of that PAH to CO₂ above the LOD was substituted for subsequent analyses. PAH emissions by compound for each stove/fuel combination are presented on a milligram per kilogram of dry fuel basis (Figure 1) and per PAH species (Table 1). PAH emissions by compound for each stove/fuel combination are also presented on a BaPe basis, calculated by multiplying the emission factor by its toxic equivalency factor (Table S5) for all PAHs that contribute more than 1% to the total BaPe (Table S2).

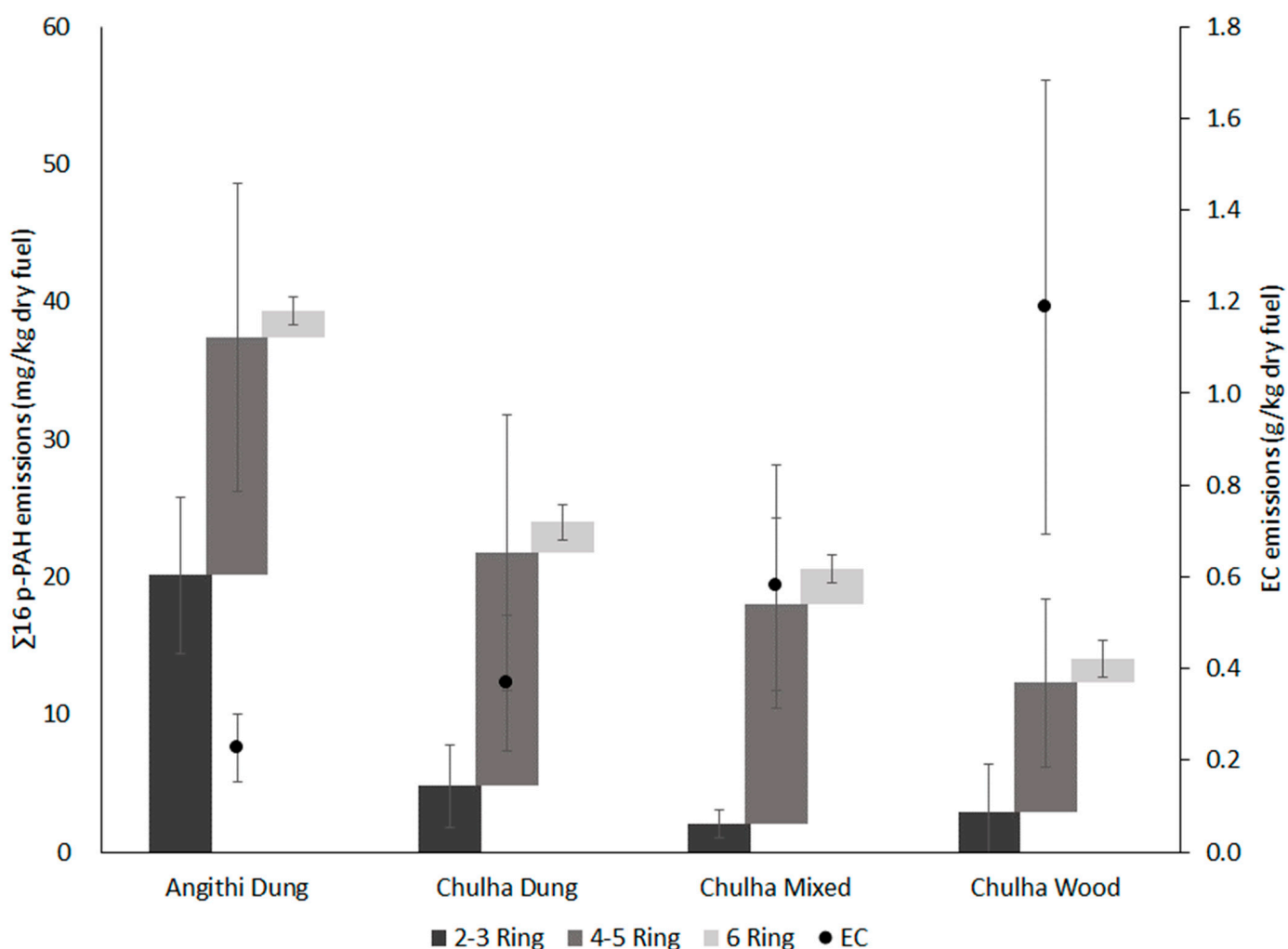


Figure 1. Average PAH emissions on a milligram of $\Sigma 16$ p-PAHs per kilogram of dry fuel separated by ring sizes as well as EC emissions on a gram per kilogram of dry fuel basis. PAH emissions are presented as a stacked bar chart with 2 or 3 rings, 4 or 5 rings, and 6 rings on a linear scale.

Table 1. PAH emissions by compound for each stove/fuel combination are presented on a milligram per kilogram of dry fuel basis.

PAH Species	Angithi Dung (n = 9)	Chulha Dung (n = 10)	Chulha Mixed (n = 12)	Chulha Wood (n = 14)
NAP	9.2 ± 1.2	3.1 ± 0.6	1.4 ± 0.3	1.7 ± 0.7
ACE/FLO	7.2 ± 1.6	1.0 ± 0.5	0.1 ± 0.1	0.7 ± 0.2
PHE	3.1 ± 0.5	0.9 ± 0.2	0.4 ± 0.1	0.4 ± 0.2
ANT	0.7 ± 0.1	0.2 ± 0.0	0.1 ± 0.0	0.1 ± 0.0
FLA	6.6 ± 1.5	4.9 ± 1.1	3.5 ± 0.4	1.5 ± 0.5
PYR	5.4 ± 1.2	4.5 ± 0.7	3.3 ± 0.5	1.7 ± 0.5
BaA/CHY	2.1 ± 0.4	2.9 ± 0.5	2.7 ± 0.3	1.4 ± 0.2
BbF/BkF	1.7 ± 0.4	3.8 ± 0.6	4.0 ± 0.4	2.9 ± 0.4
BaP	1.4 ± 0.3	2.5 ± 0.3	2.5 ± 0.3	1.9 ± 0.2
DahA	1.2 ± 0.2	1.1 ± 0.2	0.9 ± 0.1	0.7 ± 0.3
IcdP	0.7 ± 0.2	1.3 ± 0.2	1.6 ± 0.2	1.0 ± 0.1
BaPe	3.2 ± 0.6	4.3 ± 0.6	4.1 ± 0.4	3.0 ± 0.4
∑16-PAH EF	39.3 ± 5.4	26.3 ± 3.4	20.6 ± 2.2	14.0 ± 2.5

3. Results

Table 1 shows a summary of p-PAH emissions in mg per kilogram dry fuel from chulha and angithi cookstoves using dung, wood, and a mixture of both fuels. Compared to ∑16 p-PAHs emissions from dung burned in the angithi, lower emissions of ∑16 p-PAHs were observed for dung burned in the chulha ($p = 0.06$), mixed fuels in the chulha ($p < 0.01$), and wood in the chulha ($p < 0.001$). ∑16 p-PAHs emissions ranged from 75 mg/kg dry fuel in the angithi to 5 mg/kg dry in the chulha burning wood. While ∑16 p-PAHs emissions from mixed fuels in the chulha fell in between emissions from wood and dung burned independently, significant differences in emissions of ∑16 p-PAHs emission were seen between wood and dung burned in the chulha ($p = 0.045$).

In this in-field assessment, ∑16 p-PAHs emissions using the chulha were a factor of 2–3 higher than those reported for the controlled laboratory testing of wood using electric heaters, and approximately a factor of 1.5 higher than those reported for emissions from dung. The greater emissions from in-field testing is in general agreement with previous in-field assessments that reported that ∑16 p-PAHs emission from a variety of Indian cookstoves were 4–6-fold higher compared to test chambers [9]. The mean ratio of ∑16 p-PAHs to PM_{2.5} was 1.8 ± 0.8 mg p-PAHs per gram of PM_{2.5} across fuels/stoves (corresponding to a mass fraction of $0.18 \pm 0.08\%$).

Figure 1 shows ∑16 p-PAHs emissions separated by ring size alongside EC emissions. While 4- to 6-ring 16 p-PAHs were similar across the different stove and fuel combinations, the 2- and 3-ring 16 p-PAHs emissions were substantially larger from dung burning, and they were also larger in the angithi compared to chulha stoves. The fraction of 2- and 3-ring 16 p-PAHs emissions in ∑16 p-PAHs was higher in the angithi than in the chulha, as well as in the chulha with dung compared to mixed fuels (Figure 1). The ratio of 5- and 6-ring 16 p-PAHs to EC emissions was similar for the chulha (14 ± 1) and angithi (15 ± 2) when both burned dung but was a factor of 2–3 greater for dung (15 ± 2) and mixed fuels (9 ± 1) compared to wood fuels (4 ± 1). Similar to previous studies, 4- and 5-ring particulate PAHs were the dominant fraction in 16 p-PAHs in all chulha burns [37]; however, the angithi was dominated by 2- and 3-ring 16 p-PAHs and generated lower emissions of EC per kilogram of fuel burned.

4. Discussion

A better understanding of the factors that influence emissions of p-PAHs from cookstoves is necessary to better constrain variability in ∑16 p-PAHs emissions from cookstoves and also to determine sample sizes for representative measurements. ∑16 p-PAHs and

individual PAH concentrations are measured after the emissions are diluted to ambient temperature, and reported correlations reflect the partitioning equilibria of individual species at that temperature. Measurements of PAH emissions during cooking were performed in August with average ambient temperatures ranging from ~30 to ~35 °C. Cooking events conducted in different climatic regions, or during different seasons with differing ambient temperatures, would be expected to alter the amount of 16 p-PAH species, with the fraction of smaller PAHs increasing at colder ambient temperatures.

The 16 p-PAHs measured in this study are a subset of the total PAHs emitted from cooking events, and inclusion of other PAH species formed during combustion or through atmospheric reactions with parent PAH emissions [38], such as nitrated and oxygenated PAHs (nitro-PAHs and oxy-PAHs) [39], would allow for more comprehensive assessment. Strong correlations, however, have been observed between nitro- and oxy-PAHs and parent PAHs in different solid fuels used for indoor cooking [40–42], which allows for an overall estimation of emission ranges, although the relationship between parent PAHs and nitro- and oxy-PAHs is likely to vary across biomass burns. Greater abundance of compounds that are likely to be PAHs containing heterocyclic nitrogen atoms have been reported for these dung-burning compared to wood-burning stoves [33].

PM_{2.5} emissions were higher during smoldering combustion in the angithi in contrast to higher EC emissions in the chulha [33] generally in agreement with increased emissions from flaming combustion suggested in theoretical and measured papers on soot formation [43,44]. One possible explanation for the increase in Σ 16 p-PAHs for the angithi is that the placement of the cooking pot on top of the flat dung patty arrangement in the stove limits the availability of oxygen [43]. Emissions of PM_{2.5} mass were not well correlated with individual 16 p-PAHs or EC ($R^2 < 0.7$). For the PAHs that contributed over 1% of the total BaPe (Table S2), emissions of PM_{2.5} mass were particularly poorly correlated with individual PAHs ($R^2 < 0.3$), and therefore, health effects associated with PM mass or PAHs and EC are likely to have different mechanisms.

While Σ 16 p-PAHs emissions tended to decrease from dung to mixed to wood fuels in the chulha, emissions of particle bound benzo-a-pyrene (p-BaP) were correlated with total particulate PAH carcinogenicity measured on a BaPe basis ($\text{BaPe} = 1.42 * \text{BaP}$, $R^2 = 0.70$, $p < 0.001$) for all stove and fuel combinations. These relationships were especially robust for dung fuels ($R^2 = 0.88$). Emissions on a BaPe basis are slightly higher than those seen from in-home measurements of heating and cooking with yak dung in traditional stoves (0.5 and 2 mg/kg) [45]. Large increases in total PM_{2.5} emissions from the angithi mostly result in increases in lower molecular weight, less toxic, PAHs.

Recent work has reported that two high- and low-temperature VOC emission profiles explained on average 85 % of the VOC emissions during controlled burns of 15 types of natural fuel mixtures representative of fuels burned in wildfires in the western US [20]. VOC emissions did not correlate well with emissions of CO, CO₂, and NO_x mainly produced from flaming or smoldering processes, as VOC formation is controlled by pyrolysis of fuel biopolymers [20]. PAH emissions from household solid fuel use are affected by fuel type and are temperature-driven [46], resulting from the balance of two competing processes; chemical synthesis of PAHs enhanced by increasing temperature [47,48] and increasing conversion of PAHs into elemental carbon with temperature [49]. Precursor particles observed in diffusion flames can undergo conversion to carbonaceous soot in the high-temperature regions of the flame leading to the formation of aromatic clusters, and then finally EC [50]. During early flaming combustion, when temperatures are lower, a large amount of low-molecular-weight PAHs are synthesized through the hydrogen-abstraction/acetylene-addition (HACA) pathway due to oxygen restriction [51]. Wood burned in a quartz tube furnace produced large particles with diameters between 0.2 μm

and 1 μm during early flaming combustion, containing higher concentrations of low-molecular-weight PAHs indicating that PAH synthesis was the dominant process during wood combustion [51]. As temperatures increase in later burning stages, the proportion of higher-molecular-weight PAHs increases [20]. During the carbon burn phase particles within the range of 0.04 μm to 0.2 μm were emitted in lower number concentrations but with a higher concentration of higher-molecular-weight PAH emissions [51]. $\Sigma 16$ p-PAH emissions are not correlated with MCE and can actually increase despite the combustion in improved cookstoves being more thermally efficient than traditional cookstoves [52–54].

Using the emission factors reported in Fleming et al. [34], we calculated the predicted ratio of high- to low-temperature VOCs [20] given in Equation (1):

$$\frac{\text{Total Predicted VOC, High Temperature (ppbv)}}{\text{Total Predicted VOC, Low Temperature (ppbv)}} = \frac{\text{Ethyne (ppbv)}/0.039}{\text{Furan (ppbv)}/0.016} \quad (1)$$

Figure 2 shows that the ratio of 2- and 3-ring p-PAHs to total $\Sigma 16$ p-PAHs was correlated with the natural log of the ratio of high- to low-temperature VOCs ($R^2 = 0.71$). As the ratio of high- to low-temperature combustion increases, the 2- and 3-ring PAHs account for a smaller fraction of total summed particulate $\Sigma 16$ p-PAHs, which demonstrates a transition from less to more fused rings in particulate PAHs. This transition from lower- to higher-molecular-weight PAHs is most clearly demonstrated in the angithi when temperatures are lower and a large amount of low-molecular-weight PAHs are synthesized through the HACA pathway due to oxygen restriction [51]. As temperatures increase with the transition to flaming combustion in the non-angithi stoves, the proportion of high-molecular-weight PAHs increases.

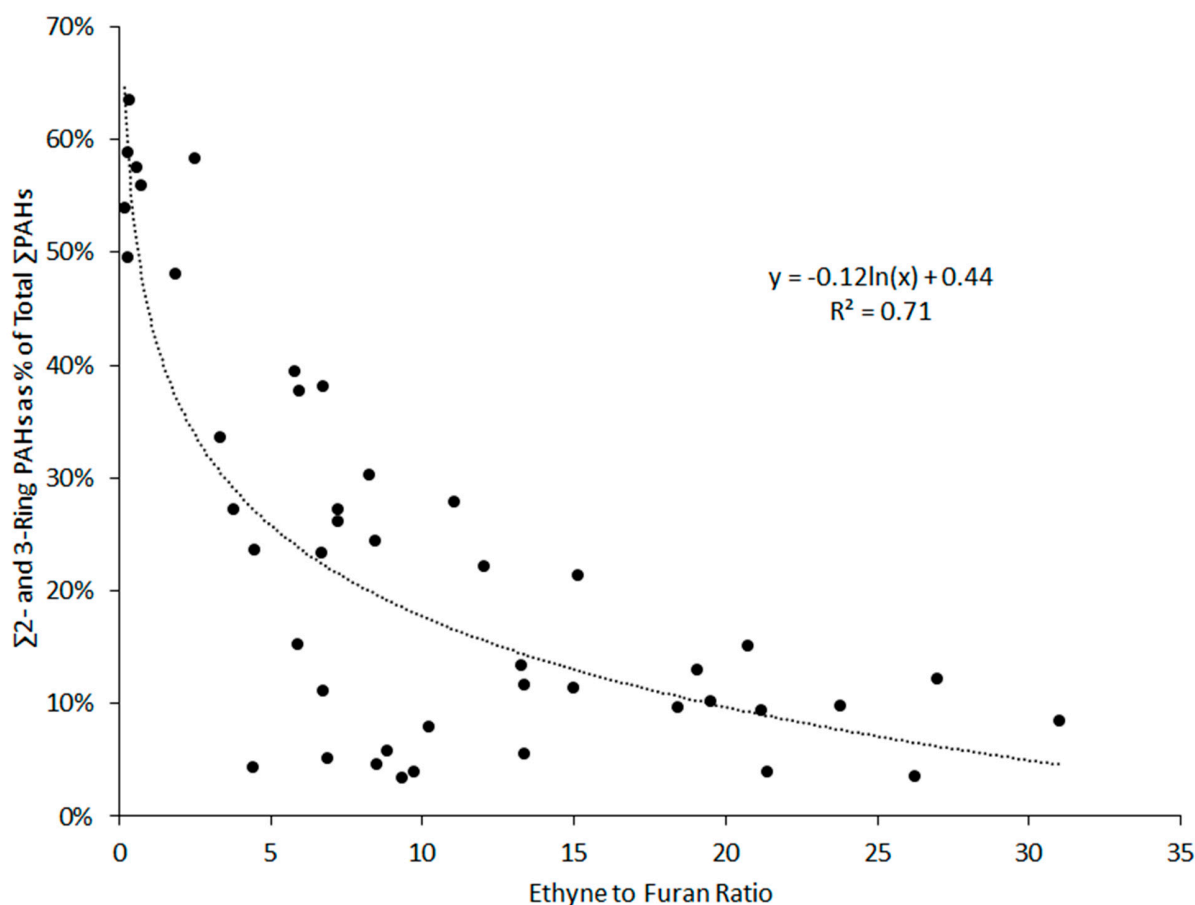


Figure 2. The ratio of 2- and 3-ring PAHs as a percent of the total summed PAHs plotted against ethyne–furan ratios.

To further explore the determinants of $\Sigma 16$ p-PAH and EC formation, Table 2 shows linear regression models for EC, $\Sigma 16$ p-PAH, and BaPe emission concentrations. $\Sigma 16$ p-PAHs and BaPe are predicted by the ratio of high- to low-temperature VOCs, fuel, and stove parameters and the removal process of EC formation as an end step in the transition from low molecular weight PAHs to high molecular weight PAHs, and then finally to soot particles. Emissions of $\Sigma 16$ p-PAHs from the chulha and angithi during tests in the village kitchen using dung and mixed fuels were not significantly correlated with MCE, and like other VOC emissions, the ratio of high- to low-temperature was a better predictor.

Table 2. Linear regression models of determinants of EC, PAH, and BaPe emission concentrations. Dependent variables are listed on the left-hand side. Models were fit either with information on PAHs as summed PAHs, the sum of 5–6-ring PAHs, BaPe, or no summed PAHs. Partial r^2 values are listed under the significant predictor variables for each model. Variables that were negatively correlated are displayed with a (-) in front of them in each model.

Dependent	Model Includes	r^2	p Value	Independent				
EC	Summed PAH	0.67	<0.001	Wood only	Mixed	(-) Angithi	Summed PAH	OC
				0.62	0.19	0.17	0.15	0.09
	Sum 5–6 ring	0.72	<0.001	Wood only	Sum 5–6 ring	OC	(-) BaPE	(-) Angithi
Summed PAH	No PAH	0.64	<0.001	MCE	CO	OC	Mixed	
				0.50	0.42	0.19	0.13	
	BaPe	0.86	<0.001	BaPe	(-) Angithi	(-) PM2.5		
5–6 ring	no BaPe	0.56	<0.001	High/low	PM2.5	Angithi		
				0.26	0.24	0.11		
	No PAH	0.68	<0.001	MCE	(-) PM2.5	(-) OC		
BaPe	Summed PAH	0.8	<0.001	Summed PAH	(-) Angithi	high/low	(-) PM2.5	
				0.71	0.19	0.12	0.12	
	No Summed PAH	0.39	<0.001	High/low	(-) Wood only	EC	(-) Mixed	
				0.32	0.21	0.12	0.10	

In regression models, while modified combustion efficiency was not predictive ($Pr>t = 0.79$), increased $PM_{2.5}$ was significantly associated with an increase in the 2- and 3-ring p-PAHs as a % of total p-PAHs ($Pr>t = 0.03$), where the best fit using Akaike’s information criterion included only the variables of $PM_{2.5}$ and the calculated ratio of high- to low-temperature VOC, given in Equation (2):

$$2\text{- and }3\text{-ring p-PAHs as \% of total p-PAHs} = 0.33 - 0.09 \times \ln(\text{Ratio of High to Low T VOCs}) + 0.004 \times PM_{2.5} \quad (2)$$

This model suggests that, as $PM_{2.5}$ emissions (g/kg dry fuel) increase the percent of lower-molecular-weight p-PAHs increases, and as the ratio of high- to low-temperature VOCs increases the p-PAHs transition towards higher-molecular-weight p-PAHs. Similarly, elemental carbon had an inverse relationship with the fractional amount of 2- and 3-ring p-PAHs. Taken together, these models indicate that MCE is a poor measure of the transition of p-PAHs from low- to high-molecular weight but that $PM_{2.5}$ and EC are significantly associated with the transition.

PAHs from biomass burning are important brown carbon chromophores [33,55] and are also directly related to emissions of EC. EC was moderately well predicted by linear regression models for these cooking events. Since EC formation occurs in the high temperature regions of the flame, the predictor variables highlight the wood combustion stoves that have the most flaming combustion as the main predictor for EC followed by synthesis of 5–6-ring compounds that are EC precursors. In general, the angithi was negatively asso-

ciated with EC as it is a lower-temperature smoldering stove, where flaming combustion is prevented.

In general, the primary predictor for $\Sigma 16$ p-PAH emissions was the ratio of high- to low-temperature VOCs, which reflects that $\Sigma 16$ p-PAHs were largely driven by the concentration of 2–3-ring p-PAHs, and thus predictors reflect the HACA synthesis pathways of 2–3-ring p-PAHs ($R^2 = 0.56$). When benzo(a)pyrene was the dependent variable, independent predictors were also driven by high- to low-temperature combustion, consistent with the models with $\Sigma 16$ p-PAHs as the dependent variable. As the ratio of high-temperature VOC to low-temperature VOC increases, there is a rise in BaPe that is consistent with larger-molecular-weight PAHs occurring as a greater proportion of total emissions. Regression models with summed $\Sigma 16$ p-PAH as the dependent variable were well predicted by benzo(a)pyrene concentrations as expected ($R^2 = 0.86$).

PAHs have a much higher thermal stability than most other VOC compounds shifting to five-ring p-PAHs during flaming combustion [56]. Predictors for the percentage of 5–6-ring p-PAH were associated with the overall combustion parameters of the cooking event (MCE), and negatively associated with PM_{2.5} and OC, which reflects greater flaming combustion that generates less organic carbon and particulate matter.

Overall, the regression models indicate that high- to low-temperature ratios are predictive of the HACA temperature-dependent formation of 2–3-ring PAHs, which drives the overall $\Sigma 16$ p-PAH concentrations in agreement with high-temperature–low-temperature formation of VOC [20]. The formation of 5–6-ring PAHs and EC were more dependent on the overall flaming combustion in the cooking event indicated by higher MCE combined with less organic carbon and particulate matter.

Use of PAH Isomer Ratios in Source Apportionment

Ratios of anthracene to the sum of anthracene and phenanthrene ($ANT/(ANT + PHE)$) are used in combustion source characterization, with lower values (usually a ratio < 0.1) reported for petroleum than those seen with biomass (approximately 0.1–0.4) [31]. In these cooking tests, all $ANT/(ANT + PHE)$ values were in the range typically seen for biomass (averages 0.18 to 0.35), with higher values for wood-only tests in the Chulha compared to other fuel stove combinations (p -values < 0.01) (Table 1). The ratios of $ANT/(ANT + PHE)$ in these cooking tests generally overlap with those in the literature for wood burning and those seen with controlled burn measurements from Chinese and Nepalese clay pots [30,31].

Ratios of fluoranthene to the sum of fluoranthene and pyrene ($FLT/(FLT + PYR)$) below 0.5 are reported for petroleum combustion, whereas values above 0.5 are reported for coal or biomass burning [30,31]. The $FLT/(FLT + PYR)$ ratio found for biomass burning in these cooking tests (averages between 0.45 and 0.55, Table 3) overlapped the ranges for petroleum combustion source signatures [27], indicating that these emissions could be incorrectly ascribed to petroleum combustion rather than domestic household biomass combustion. Further, the $FLT/(FLT + PYR)$ ratio decreased in this study going from dung to wood fuels (borderline significant; $Pr > F = 0.15$), indicating that the degree to which cooking sources are misrepresented as fossil fuel burning can be dependent on the specific fuel and stove combination for biomass cooking fuels. While all dung-burning tests, including mixed fuels, had average $FLT/(FLT + PYR)$ ratios over 0.5, the wood-only tests in the chulha had an average of 0.46 (arithmetic mean; geomean = 0.45). While the $FLT/(FLT + PYR)$ ratios observed in these in-field cooking tests are lower than controlled burns using Chinese and Nepalese clay pots burning wood [31], ratios for wood combustion in traditional stoves have ranged between 0.43 and 0.74 [30], which also indicate overlapping source signature ranges and that household cooking may be incorrectly ascribed to petroleum combustion.

Table 3. Arithmetic means and standard deviations of PAH isomer ratios used in source apportionment studies from dung, mixed fuels, and wood only from in-field cooking tests using the angithi and chulha. Ratios from Chinese and Nepalese clay pots from [57] are for particulate matter only from 8 kg wood over a 4 h burn.

PAH Isomer Ratio	Wood in Chulha	Mixed Fuel in Chulha	Dung in Chulha	Dung in Angithi	Wood in Chinese Clay [57]	Wood in Nepalese Clay [57]
ANT/(ANT + PHE)	0.35 ± 0.13	0.22 ± 0.06	0.18 ± 0.06	0.18 ± 0.01	0.25	0.07
FLT/(FLT + PYR)	0.46 ± 0.08	0.53 ± 0.06	0.51 ± 0.16	0.55 ± 0.02	0.71	0.67
FLT/PYR	0.90 ± 0.26	1.14 ± 0.29	1.15 ± 0.46	1.22 ± 0.08	2.4	2

5. Summary

In this paper, quantitative assessment of 16 particle-phase polycyclic aromatic hydrocarbons (PAHs) in 45 in-field cooking events using wood, bovine dung, and these two fuels mixed together in two types of stoves indicated that Σ 16 p-PAH emissions were greatest from dung-based cooking events as a result of high emissions of 2–3-ring PAHs. Wood fuels showed the lowest emissions with mixed fuels between dung and wood, and emissions from wood-fired cooking events were higher than in laboratory studies. Elemental carbon emissions were closely linked to the higher molecular weight of 5- and 6-ring PAHs and the fuel type and stove types used in this study. In general, regression models indicate that ethyne–furan ratios are predictive of the HACA temperature-dependent formation of 2–3-ring p-PAHs, which drives overall Σ 16 p-PAH concentrations. Formation of 5–6-ring p-PAHs and EC were more dependent on the overall flaming combustion performance in the cooking event. PAH isomer ratios used in source apportionment were shown to vary between dung and wood burns and the ratio of fluoranthene to the sum of fluoranthene and pyrene (FLU/FLU + PYR) typically used for fossil-fuel burning overlapped with the mean value for our wood-only testing.

Supplementary Materials: The following supporting information can be downloaded at <https://www.mdpi.com/article/10.3390/atmos16020121/s1>, Figure S1: Chulha (left) and angithi (right) used during this project. The angithi is loaded with smoldering cow dung patties and used to simmer animal feed; Figure S2: Chulha stove using brushwood; Figure S3: Average particulate PAH emissions by species for the angithi stove (brown), chulha with mixed fuels (green), chulha with dung (blue), and chulha with wood (orange). Error bars show one standard error of the mean. Benzo(b) and Benzo(k)fluoranthene are summed together; Figure S4: Average particulate PAH emissions by BaP-equivalency for each species for the angithi stove (brown), chulha with mixed fuels (green), chulha with dung (blue), and chulha with wood (orange). Error bars show one standard error of the mean. Benzo(b) and Benzo(k)fluoranthene are summed together; Table S1: Percentage of samples above LoD for all samples where PAHs were detected; Table S2: PAH emissions by compound for each stove/fuel combination are presented on a milligram BaPe per kilogram of dry fuel basis. The final column lists the percentage of total mgTEF that the Σ PAHs add up to. Only the measured compounds that contribute over 1% of total calculated BaPe are listed here; Table S3: Concentrations of individual PAH species in standard reference material 1648a, urban particulate matter, measured in this study by HPLC-FLD and values reported by the manufacturer via GC-Soxhlet/pressurized fluid extraction; Table S4: Recovery (in %) of individual PAH species on quartz Filters (47 mm) spiked with 1 mL of 50 ng/mL PAH Standard Mix, extracted and analyzed by HPLC-FLD following NIOSH Method 5506; Table S5: Toxic equivalency factors for individual PAH species presented in this paper.

Author Contributions: Conceptualization, R.D.E. and R.M.W.; methodology, N.S. and S.A.N.; validation, N.S., R.M.W. and R.D.E.; formal analysis, R.D.E. and R.M.W.; field investigation, R.M.W. and R.D.E.; writing—original draft preparation, R.M.W. and R.D.E.; writing—review and editing, R.D.E., N.S., R.M.W., S.A.N. and A.P.; project administration, N.K.A. and A.P.; funding acquisition, R.D.E. All authors have read and agreed to the published version of the manuscript.

Funding: This research was funded by Environmental Protection Agency. The EPA STAR grant R835425 Impacts of household sources on outdoor pollution at village and regional scales in India.

Data Availability Statement: The data supporting the conclusions of this article will be made available by the authors on request.

Acknowledgments: This research was supported by EPA STAR grant R835425 impacts of household sources on outdoor pollution at village and regional scales in India. The contents are solely the responsibility of the authors and do not necessarily represent the official views of the US EPA. The US EPA does not endorse the purchase of any commercial products or services mentioned in the publication. Great thanks go to Donald Blake and the other members of their lab for their work quantifying gas-phase emissions as part of this grant.

Conflicts of Interest: Norbert Staimer is affiliated with BioAssayPro LLC. The paper reflects the views of the scientists and not the company. The authors declare no conflict of interest.

References

1. Edwards, R.; Princevac, M.; Weltman, R.; Ghasemian, M.; Arora, N.K.; Bond, T. Modeling emission rates and exposures from outdoor cooking. *Atmos. Environ.* **2017**, *164*, 50–60. [[CrossRef](#)]
2. Edwards, R.; Bond, T.; Smith, K.R. Characterization of emissions from small, variable solid fuel combustion sources for determining global emissions and climate impact. In *Final Project Report EPA STAR 83503601*; United States Environmental Protection Agency: Washington DC, USA, 2017.
3. Rooney, B.; Zhao, R.; Wang, Y.; Bates, K.H.; Pillarisetti, A.; Sharma, S.; Kundu, S.; Bond, T.C.; Lam, N.L.; Ozaltun, B. Impacts of household sources on air pollution at village and regional scales in India. *Atmos. Chem. Phys.* **2019**, *19*, 7719–7742. [[CrossRef](#)]
4. Smith, K.R.; McCracken, J.P.; Weber, M.W.; Hubbard, A.; Jenny, A.; Thompson, L.M.; Balmes, J.; Diaz, A.; Arana, B.; Bruce, N. Effect of reduction in household air pollution on childhood pneumonia in Guatemala (RESPIRE): A randomised controlled trial. *Lancet* **2011**, *378*, 1717–1726. [[CrossRef](#)] [[PubMed](#)]
5. Låg, M.; Øvrevik, J.; Refsnes, M.; Holme, J.A. Potential role of polycyclic aromatic hydrocarbons in air pollution-induced non-malignant respiratory diseases. *Respir. Res.* **2020**, *21*, 1–22. [[CrossRef](#)]
6. Luderer, U.; Lim, J.; Ortiz, L.; Nguyen, J.D.; Shin, J.H.; Allen, B.D.; Liao, L.S.; Malott, K.; Perraud, V.; Wingen, L.M. Exposure to environmentally relevant concentrations of ambient fine particulate matter (PM_{2.5}) depletes the ovarian follicle reserve and causes sex-dependent cardiovascular changes in apolipoprotein E null mice. *Part. Fibre Toxicol.* **2022**, *19*, 5. [[CrossRef](#)] [[PubMed](#)]
7. Bhargava, A.; Khanna, R.; Bhargava, S.; Kumar, S. Exposure risk to carcinogenic PAHs in indoor-air during biomass combustion whilst cooking in rural India. *Atmos. Environ.* **2004**, *38*, 4761–4767. [[CrossRef](#)]
8. Ambade, B.; Kumar, A.; Sahu, L.K. Characterization and health risk assessment of particulate bound polycyclic aromatic hydrocarbons (PAHs) in indoor and outdoor atmosphere of Central East India. *Environ. Sci. Pollut. Res.* **2021**, *28*, 56269–56280. [[CrossRef](#)] [[PubMed](#)]
9. Verma, M.; Pervez, S.; Chow, J.C.; Majumdar, D.; Watson, J.G.; Pervez, Y.F.; Deb, M.K.; Shrivastava, K.; Jain, V.K.; Khan, N.A. Assessing the magnitude of PM_{2.5} polycyclic aromatic hydrocarbon emissions from residential solid fuel combustion and associated health hazards in South Asia. *Atmos. Pollut. Res.* **2021**, *12*, 101142. [[CrossRef](#)]
10. Nisbet, I.C.; Lagoy, P.K. Toxic equivalency factors (TEFs) for polycyclic aromatic hydrocarbons (PAHs). *Regul. Toxicol. Pharmacol.* **1992**, *16*, 290–300. [[CrossRef](#)]
11. Gustafson, P.; Barregard, L.; Strandberg, B.; Sällsten, G. The impact of domestic wood burning on personal, indoor and outdoor levels of 1,3-butadiene, benzene, formaldehyde and acetaldehyde. *J. Environ. Monit.* **2007**, *9*, 23–32. [[CrossRef](#)] [[PubMed](#)]
12. Wei, S.; Shen, G.; Zhang, Y.; Xue, M.; Xie, H.; Lin, P.; Chen, Y.; Wang, X.; Tao, S. Field measurement on the emissions of PM, OC, EC and PAHs from indoor crop straw burning in rural China. *Environ. Pollut.* **2014**, *184*, 18–24. [[CrossRef](#)] [[PubMed](#)]
13. Mukhopadhyay, K.; Chakraborty, D.; Natarajan, S.; Sambandam, S.; Balakrishnan, K. Monitoring of polycyclic aromatic hydrocarbons emitted from kerosene fuel burning and assessment of health risks among women in selected rural and urban households of South India. *Environ. Geochem. Health* **2023**, *45*, 1445–1459. [[CrossRef](#)]
14. Weltman, R.M.; Edwards, R.D.; Fleming, L.T.; Yadav, A.; Weyant, C.L.; Rooney, B.; Seinfeld, J.H.; Arora, N.K.; Bond, T.C.; Nizkorodov, S.A. Emissions measurements from household solid fuel use in Haryana, India: Implications for climate and health co-benefits. *Environ. Sci. Technol.* **2021**, *55*, 3201–3209. [[CrossRef](#)]
15. Thompson, R.J.; Li, J.; Weyant, C.L.; Edwards, R.; Lan, Q.; Rothman, N.; Hu, W.; Dang, J.; Dang, A.; Smith, K.R. Field emission measurements of solid fuel stoves in Yunnan, China demonstrate dominant causes of uncertainty in household emission inventories. *Environ. Sci. Technol.* **2019**, *53*, 3323–3330. [[CrossRef](#)] [[PubMed](#)]

16. Verma, A.R.; Tiwari, R.; Verma, M.K.; Kumar, H. Practical Evaluation Approach of a Typical Biomass Cookstove. In *Bioenergy Engineering*; CRC Press: Boca Raton, FL, USA, 2021; pp. 209–229.
17. Adhikari, S.; Mahapatra, P.S.; Pokheral, C.P.; Puppala, S.P. Cookstove smoke impact on ambient air quality and probable consequences for human health in rural locations of southern Nepal. *Int. J. Environ. Res. Public Health* **2020**, *17*, 550. [[CrossRef](#)] [[PubMed](#)]
18. Du, W.; Yun, X.; Chen, Y.; Zhong, Q.; Wang, W.; Wang, L.; Qi, M.; Shen, G.; Tao, S. PAHs emissions from residential biomass burning in real-world cooking stoves in rural China. *Environ. Pollut.* **2020**, *267*, 115592. [[CrossRef](#)]
19. Du, W.; Wang, J.; Zhuo, S.; Zhong, Q.; Wang, W.; Chen, Y.; Wang, Z.; Mao, K.; Huang, Y.; Shen, G. Emissions of particulate PAHs from solid fuel combustion in indoor cookstoves. *Sci. Total Environ.* **2021**, *771*, 145411. [[CrossRef](#)] [[PubMed](#)]
20. Sekimoto, K.; Koss, A.R.; Gilman, J.B.; Selimovic, V.; Coggon, M.M.; Zarzana, K.J.; Yuan, B.; Lerner, B.M.; Brown, S.S.; Warneke, C. High-and low-temperature pyrolysis profiles describe volatile organic compound emissions from western US wildfire fuels. *Atmos. Chem. Phys.* **2018**, *18*, 9263–9281. [[CrossRef](#)]
21. Maxwell, D.; Gudka, B.; Jones, J.; Williams, A. Emissions from the combustion of torrefied and raw biomass fuels in a domestic heating stove. *Fuel Process. Technol.* **2020**, *199*, 106266. [[CrossRef](#)]
22. Reizer, E.; Viskolcz, B.; Fiser, B. Formation and growth mechanisms of polycyclic aromatic hydrocarbons: A mini-review. *Chemosphere* **2021**, *291*, 132793. [[CrossRef](#)]
23. Tobiszewski, M. Application of diagnostic ratios of PAHs to characterize the pollution emission sources. In Proceedings of the 5th International Conference on Environmental Science and Technology, Gdansk, Poland, 14–16 May 2014; pp. 41–44.
24. Verma, R.; Patel, K.S.; Verma, S.K. Indoor polycyclic aromatic hydrocarbon concentration in central India. *Polycycl. Aromat. Compd.* **2016**, *36*, 152–168. [[CrossRef](#)]
25. Rajput, P.; Sarin, M.; Sharma, D.; Singh, D. Atmospheric polycyclic aromatic hydrocarbons and isomer ratios as tracers of biomass burning emissions in Northern India. *Environ. Sci. Pollut. Res.* **2014**, *21*, 5724–5729. [[CrossRef](#)] [[PubMed](#)]
26. Rajput, P.; Sarin, M.; Rengarajan, R.; Singh, D. Atmospheric polycyclic aromatic hydrocarbons (PAHs) from post-harvest biomass burning emissions in the Indo-Gangetic Plain: Isomer ratios and temporal trends. *Atmos. Environ.* **2011**, *45*, 6732–6740. [[CrossRef](#)]
27. Chen, K.-S.; Wang, H.-K.; Peng, Y.-P.; Wang, W.-C.; Chen, C.-H.; Lai, C.-H. Effects of open burning of rice straw on concentrations of atmospheric polycyclic aromatic hydrocarbons in Central Taiwan. *J. Air Waste Manag. Assoc.* **2008**, *58*, 1318–1327. [[CrossRef](#)] [[PubMed](#)]
28. Singh, D.; Gadi, R.; Mandal, T. Emissions of polycyclic aromatic hydrocarbons in the atmosphere: An indian perspective. *Hum. Ecol. Risk Assess.* **2010**, *16*, 1145–1168. [[CrossRef](#)]
29. Shen, H.; Huang, Y.; Wang, R.; Zhu, D.; Li, W.; Shen, G.; Wang, B.; Zhang, Y.; Chen, Y.; Lu, Y. Global atmospheric emissions of polycyclic aromatic hydrocarbons from 1960 to 2008 and future predictions. *Environ. Sci. Technol.* **2013**, *47*, 6415–6424. [[CrossRef](#)]
30. Shen, G.; Wang, W.; Yang, Y.; Ding, J.; Xue, M.; Min, Y.; Zhu, C.; Shen, H.; Li, W.; Wang, B. Emissions of PAHs from indoor crop residue burning in a typical rural stove: Emission factors, size distributions, and gas–particle partitioning. *Environ. Sci. Technol.* **2011**, *45*, 1206–1212. [[CrossRef](#)]
31. Yunker, M.B.; Macdonald, R.W.; Vingarzan, R.; Mitchell, R.H.; Goyette, D.; Sylvestre, S. PAHs in the Fraser River basin: A critical appraisal of PAH ratios as indicators of PAH source and composition. *Org. Geochem.* **2002**, *33*, 489–515. [[CrossRef](#)]
32. Akyüz, M.; Çabuk, H. Gas–particle partitioning and seasonal variation of polycyclic aromatic hydrocarbons in the atmosphere of Zonguldak, Turkey. *Sci. Total Environ.* **2010**, *408*, 5550–5558. [[CrossRef](#)] [[PubMed](#)]
33. Fleming, L.T.; Lin, P.; Laskin, A.; Laskin, J.; Weltman, R.; Edwards, R.D.; Arora, N.K.; Yadav, A.; Meinardi, S.; Blake, D.R. Molecular composition of particulate matter emissions from dung and brushwood burning household cookstoves in Haryana, India. *Atmos. Chem. Phys.* **2018**, *18*, 2461–2480. [[CrossRef](#)]
34. Fleming, L.T.; Weltman, R.; Yadav, A.; Edwards, R.D.; Arora, N.K.; Pillarisetti, A.; Meinardi, S.; Smith, K.R.; Blake, D.R.; Nizkorodov, S.A. Emissions from village cookstoves in Haryana, India, and their potential impacts on air quality. *Atmos. Chem. Phys.* **2018**, *18*, 15169–15182. [[CrossRef](#)]
35. Weinstein, J.R.; Asteria-Peñaloza, R.; Diaz-Artiga, A.; Davila, G.; Hammond, S.K.; Ryde, I.T.; Meyer, J.N.; Benowitz, N.; Thompson, L.M. Exposure to polycyclic aromatic hydrocarbons and volatile organic compounds among recently pregnant rural Guatemalan women cooking and heating with solid fuels. *Int. J. Hyg. Environ. Health* **2017**, *220*, 726–735. [[CrossRef](#)] [[PubMed](#)]
36. Albinet, A.; Tomaz, S.; Lestremau, F. A really quick easy cheap effective rugged and safe (QuEChERS) extraction procedure for the analysis of particle-bound PAHs in ambient air and emission samples. *Sci. Total Environ.* **2013**, *450*, 31–38. [[CrossRef](#)] [[PubMed](#)]
37. Gadi, R.; Singh, D.; Saud, T.; Mandal, T.; Saxena, M. Emission estimates of particulate PAHs from biomass fuels used in Delhi, India. *Hum. Ecol. Risk Assess. Int. J.* **2012**, *18*, 871–887. [[CrossRef](#)]
38. Lee, Y.-Y.; Hsieh, Y.-K.; Huang, B.-W.; Mutuku, J.K.; Chang-Chien, G.-P.; Huang, S. An Overview: PAH and Nitro-PAH Emission from the Stationary Sources and their Transformations in the Atmosphere. *Aerosol Air Qual. Res.* **2022**, *22*, 220164. [[CrossRef](#)]

39. Zhang, Y.; Shen, Z.; Sun, J.; Zhang, L.; Zhang, B.; Zou, H.; Zhang, T.; Ho, S.S.H.; Chang, X.; Xu, H. Parent, alkylated, oxygenated and nitrated polycyclic aromatic hydrocarbons in PM_{2.5} emitted from residential biomass burning and coal combustion: A novel database of 14 heating scenarios. *Environ. Pollut.* **2021**, *268*, 115881. [[CrossRef](#)] [[PubMed](#)]
40. Shen, G.; Tao, S.; Wang, W.; Yang, Y.; Ding, J.; Xue, M.; Min, Y.; Zhu, C.; Shen, H.; Li, W.; et al. Emission of Oxygenated Polycyclic Aromatic Hydrocarbons from Indoor Solid Fuel Combustion. *Environ. Sci. Technol.* **2011**, *45*, 3459–3465. [[CrossRef](#)]
41. Shen, G.; Wei, S.; Zhang, Y.; Wang, R.; Wang, B.; Li, W.; Shen, H.; Huang, Y.; Chen, Y.; Chen, H. Emission of oxygenated polycyclic aromatic hydrocarbons from biomass pellet burning in a modern burner for cooking in China. *Atmos. Environ.* **2012**, *60*, 234–237. [[CrossRef](#)] [[PubMed](#)]
42. Shen, G.; Tao, S.; Wei, S.; Zhang, Y.; Wang, R.; Wang, B.; Li, W.; Shen, H.; Huang, Y.; Chen, Y. Emissions of parent, nitro, and oxygenated polycyclic aromatic hydrocarbons from residential wood combustion in rural China. *Environ. Sci. Technol.* **2012**, *46*, 8123–8130. [[CrossRef](#)]
43. Orasche, J.; Schnelle-Kreis, J.; Schön, C.; Hartmann, H.; Ruppert, H.; Arteaga-Salas, J.M.; Zimmermann, R. Comparison of emissions from wood combustion. Part 2: Impact of combustion conditions on emission factors and characteristics of particle-bound organic species and polycyclic aromatic hydrocarbon (PAH)-related toxicological potential. *Energy Fuels* **2013**, *27*, 1482–1491. [[CrossRef](#)]
44. Lea-Langton, A.; Baeza-Romero, M.; Boman, G.; Brooks, B.; Wilson, A.; Atika, F.; Bartle, K.; Jones, J.; Williams, A. A study of smoke formation from wood combustion. *Fuel Process. Technol.* **2015**, *137*, 327–332. [[CrossRef](#)]
45. Sun, J.; Shen, Z.; Zhang, B.; Zhang, L.; Zhang, Y.; Zhang, Q.; Wang, D.; Huang, Y.; Liu, S.; Cao, J. Chemical source profiles of particulate matter and gases emitted from solid fuels for residential cooking and heating scenarios in Qinghai-Tibetan Plateau. *Environ. Pollut.* **2021**, *285*, 117503. [[CrossRef](#)] [[PubMed](#)]
46. L'Orange, C.; Volckens, J.; DeFoort, M. Influence of stove type and cooking pot temperature on particulate matter emissions from biomass cook stoves. *Energy Sustain. Dev.* **2012**, *16*, 448–455. [[CrossRef](#)]
47. Shukla, B.; Koshi, M. A highly efficient growth mechanism of polycyclic aromatic hydrocarbons. *Phys. Chem. Chem. Phys.* **2010**, *12*, 2427–2437. [[CrossRef](#)] [[PubMed](#)]
48. Pergal, M.M.; Tesic, Z.L.; Popović, A.R. Polycyclic aromatic hydrocarbons: Temperature driven formation and behavior during coal combustion in a coal-fired power plant. *Energy Fuels* **2013**, *27*, 6273–6278. [[CrossRef](#)]
49. Thomas, S.; Wornat, M.J. The effects of oxygen on the yields of polycyclic aromatic hydrocarbons formed during the pyrolysis and fuel-rich oxidation of catechol. *Fuel* **2008**, *87*, 768–781. [[CrossRef](#)]
50. Santamaria, A.; Yang, N.; Eddings, E.; Mondragon, F. Chemical and morphological characterization of soot and soot precursors generated in an inverse diffusion flame with aromatic and aliphatic fuels. *Combust. Flame* **2010**, *157*, 33–42. [[CrossRef](#)]
51. Han, Y.; Chen, Y.; Feng, Y.; Song, W.; Cao, F.; Zhang, Y.; Li, Q.; Yang, X.; Chen, J. Different formation mechanisms of PAH during wood and coal combustion under different temperatures. *Atmos. Environ.* **2020**, *222*, 117084. [[CrossRef](#)]
52. Jetter, J.; Zhao, Y.; Smith, K.R.; Khan, B.; Yelverton, T.; DeCarlo, P.; Hays, M.D. Pollutant emissions and energy efficiency under controlled conditions for household biomass cookstoves and implications for metrics useful in setting international test standards. *Environ. Sci. Technol.* **2012**, *46*, 10827–10834. [[CrossRef](#)]
53. Zhi, G.; Peng, C.; Chen, Y.; Liu, D.; Sheng, G.; Fu, J. Deployment of coal briquettes and improved stoves: Possibly an option for both environment and climate. *Environ. Sci. Technol.* **2009**, *43*, 5586–5591. [[CrossRef](#)]
54. Just, B.; Rogak, S.; Kandlikar, M. Characterization of ultrafine particulate matter from traditional and improved biomass cookstoves. *Environ. Sci. Technol.* **2013**, *47*, 3506–3512. [[CrossRef](#)] [[PubMed](#)]
55. Yuan, W.; Huang, R.-J.; Yang, L.; Guo, J.; Chen, Z.; Duan, J.; Wang, T.; Ni, H.; Han, Y.; Li, Y. Characterization of the light-absorbing properties, chromophore composition and sources of brown carbon aerosol in Xi'an, northwestern China. *Atmos. Chem. Phys.* **2020**, *20*, 5129–5144. [[CrossRef](#)]
56. Pagels, J.; Dutcher, D.D.; Stolzenburg, M.R.; McMurry, P.H.; Galli, M.E.; Gross, D.S. Fine-particle emissions from solid biofuel combustion studied with single-particle mass spectrometry: Identification of markers for organics, soot, and ash components. *J. Geophys. Res. Atmos.* **2013**, *118*, 859–870. [[CrossRef](#)]
57. Oanh, N.K.; Albina, D.; Ping, L.; Wang, X. Emission of particulate matter and polycyclic aromatic hydrocarbons from select cookstove-fuel systems in Asia. *Biomass Bioenergy* **2005**, *28*, 579–590. [[CrossRef](#)]

Disclaimer/Publisher's Note: The statements, opinions and data contained in all publications are solely those of the individual author(s) and contributor(s) and not of MDPI and/or the editor(s). MDPI and/or the editor(s) disclaim responsibility for any injury to people or property resulting from any ideas, methods, instructions or products referred to in the content.